

Feature-based Non-rigid Volume Registration of Serial Coronary CT Angiography

Jonghye Woo¹, Byung-Woo Hong², Damini Dey⁴, Victor Cheng⁴, Amit Ramesh⁴, Ganesh Sundaramoorthi³, C. -C. Jay Kuo¹, Daniel S. Berman, Guido Germano⁴ and Piotr J. Slomka⁴

¹Department of Electrical Engineering, University of Southern California, Los Angeles, CA 90089-2564, USA

²School of Computer Science and Engineering, Chung-Ang University, Seoul, 156-756, Korea

³Computer Science, University of California, Los Angeles, 90095, CA, USA

⁴Departments of Imaging and Medicine, Cedars-Sinai Medical Center, Los Angeles, 90048, CA, USA

ABSTRACT

Coronary CT angiography (CTA) with multi-slice helical scanners is becoming the integral part of major diagnostic pathways for coronary artery disease. In addition, coronary CTA has demonstrated substantial potential in quantitative coronary plaque characterization. If serial comparisons of plaque progression or regression are to be made, accurate 3D volume registration of these volumes would be particularly useful. In this work, we propose a coronary CTA volume registration of the paired coronary CTA scans using feature-based non-rigid volume registration. We achieve this with a combined registration strategy, which uses the global rigid registration as an initialization, followed by local registration using non-rigid volume registration with a volume preserving constraint. We exploit the extracted coronary trees to help localize and emphasize the region of interest as unnecessary regions hinder registration process, which results in wrong registration result. The extracted binary masks of each coronary tree may not be the same due to initial segmentation errors, which could lead to subsequent bias in the registration process. Therefore we utilize a blur mask which is generated by convolving the Gaussian function with the binary coronary tree mask to include the neighboring vessel region into account. A volume preserving constraint is imposed so that the total volume of the binary mask before and after co-registration remains constant. To validate the proposed method, we perform experiments with data from 3 patients with available serial CT scans (6 scans in total) and measure the distance of anatomical landmarks between the registered serial scans of the same patient.

Keywords: Nonlinear registration, Image registration, Volume-preserving constraint, Coronary CT angiography (CTA)

1. INTRODUCTION

Coronary CT angiography (CTA) has recently become an effective clinical tool for non-invasive assessment of coronary arteries due to the introduction of 64-slice CT scanners with fast gantry rotation times [1; 2]. coronary CTA has the potential to become an integral part of popular diagnostic pathways for CAD. Nonetheless, current coronary CTA state-of-the-art techniques which are used to detect coronary plaques and assess their characteristics are usually manual, subjective, and associated with high observer variability [3]. Thus accurate and robust quantification of plaque changes including progression and regression from the paired coronary CTA scans would be desirable. To this end, accurate serial volume registration of high resolution coronary data is of great importance and is the focus of this work.

Nonlinear registration refers to the process of estimating nonlinear mapping function which transforms each point in one image to a point in target image and it has been one of main subjects in medical imaging with many applications in image-guided surgery [4], multi-modality registration [5-7] and motion correction and determination [8]. Especially nonlinear registration plays a crucial role in detecting structural changes over time as well.

While many registration techniques have been proposed for the application of measuring volume or shape changes in MRI scans [9-12] as well as in serial nonlinear registration of CT [13-17]; to the best of our knowledge, none of this techniques have been applied to coronary CTA imaging. This imaging technique is particularly challenging because of the motion and the small size of the coronary arteries (2-3 mm in the diameter). In addition, plaque progression is particularly challenging because areas with plaque changes consist of small local changes within coronary arteries. Correspondingly, accurate registration for assessment of serial coronary CTA is challenging because the algorithm must deform the source image in the coronary artery region while preserving true plaque changes, and there can be significant intensity differences between the two data sets due to acquisition at different times.

In this paper, we propose a novel fully-automatic serial registration method for coronary CTA scans using a dense nonparametric registration model via diffeomorphism. It has advantages of using a binary feature mask obtained by segmentation of coronary artery and nonlinear registration. To remedy the difficulties mentioned above, we introduce a 3D blur mask that takes the coronary artery region and its neighboring region into consideration and a volume preserving constraint that is used to guarantee a constant volume before and after the registration.

2. METHODS

In our registration scheme, we consider two transformations that consist of a global displacement and a local deformation. The global displacement is initially obtained by the optimal rigid transformation and the local deformation is subsequently obtained by the optimal non-rigid transformation that is represented by diffeomorphism with a volume-preserving constraint. In this process, we utilize coronary trees that are initially obtained by the existing workstation software (Siemens, Circulation workstation) and use them as initial feature masks in the registration process. The binary 3D map which contain voxels with most of the coronary vessels, obtained by the segmentation is subsequently convolved with a Gaussian kernel to ensure that the bias of the registration due to the use of pre-segmented binary maps become weaker. The weaker feature masks called “blur mask” is useful for guiding the registration process.

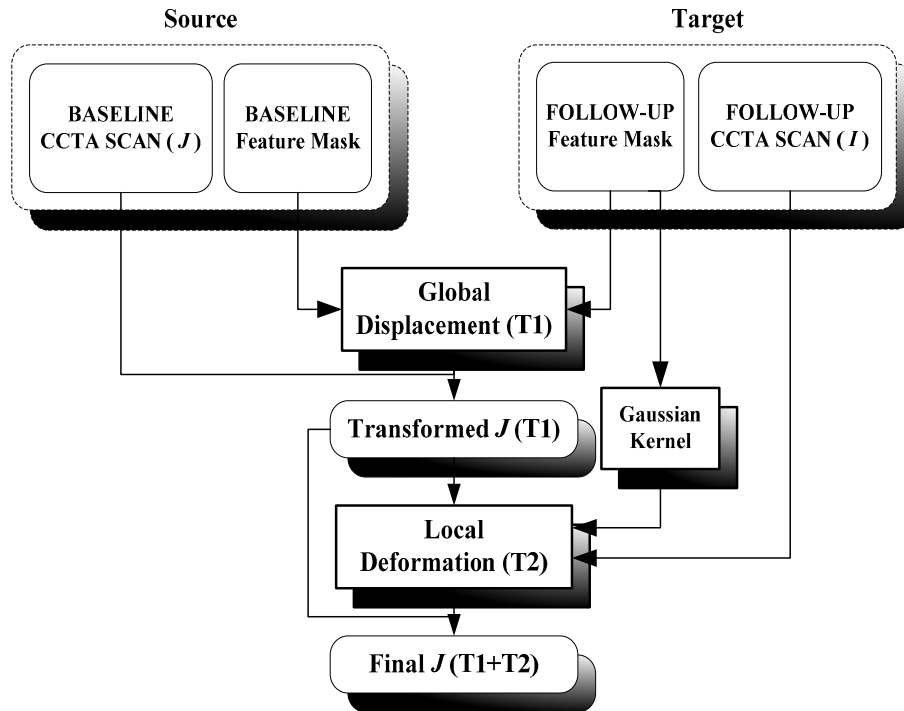


Fig. 1. Overview of image registration process

2.1. Energy Formulation for Feature-based Non-rigid Registration with Volume Constraint

Let Ω be an open and bounded domain in \mathfrak{R}^n , for arbitrary n . Let $I, J : \Omega \rightarrow \mathfrak{R}$ be two volumes to be registered. Then the goal of registration is to find the transformation $h : \Omega \rightarrow \Omega$ that maps the source volume J into correspondence with target volume I .



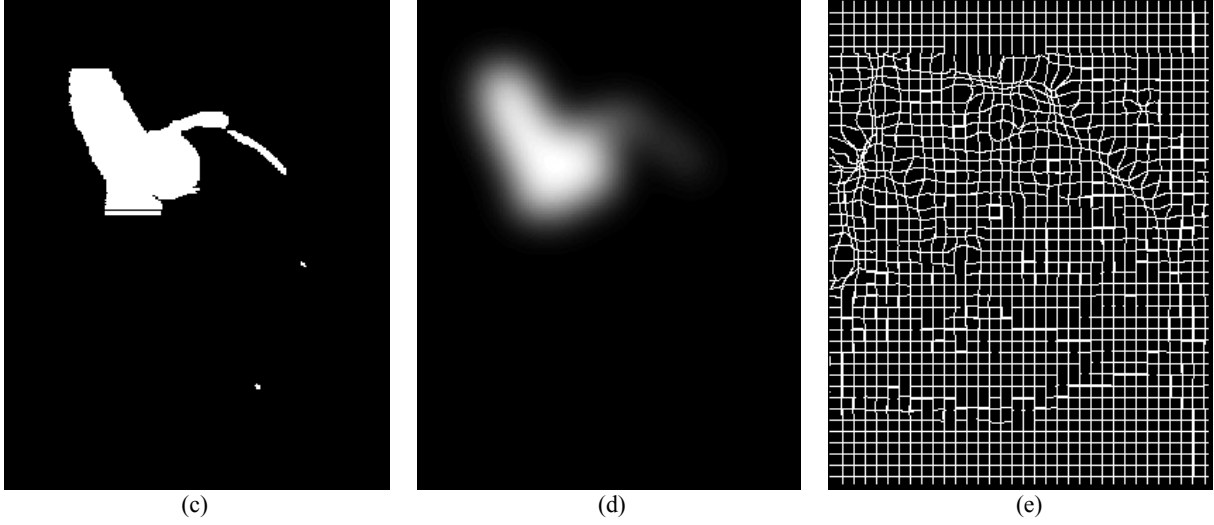


Fig. 2. Example of registration results from one patient with 2 serial scans. A slice obtained from coronal orientation is shown in the top row with the resulting baseline volumes of rigid transformation (a) and the follow-up volume (b). To emphasize region of interest, we obtained binary mask (c) and blur mask (d) by convolving Gaussian kernel. The registration result is represented by the deformation field (e) that shows a non-rigid deformation from the baseline volume to follow-up volume.

2.1.1. Blur mask

$W_I, W_J : \Omega \rightarrow \mathfrak{R}^+$ are binary masks of coronary trees in target volume I and source volume J , respectively which are obtained previously using commercial Siemens software. Now we define “blur mask” w_I and w_J in the following way:

$$w_I = W_I * G_\sigma \text{ and } w_J = W_J * G_\sigma,$$

where G_σ is a Gaussian filter with standard deviation σ that is chosen according to the reliability of the segmentation results. We will apply blur mask as a weighting function for the registration and this provides a way to emphasize the local neighborhood of regions of interest in registration.

2.1.2 Energy Formulation of Local Deformation

Our proposed energy functional for local deformation consists of data fidelity term, regularization, and a volume-preserving constraint as follows:

$$E = \alpha \int_{\Omega} w_I(x) \|I(x) - J \circ h(x)\|^2 dx + \beta \int_{\Omega} \|\nabla h(x)\|^2 dx + \lambda \left(\int_{\Omega} w_J \circ h(x) dx - \int_{\Omega} w_J(x) dx \right)^2$$

where $\Omega \subset \mathfrak{R}^2$, $h : \Omega \rightarrow \Omega$ is a diffeomorphism, $I, J : \Omega \rightarrow \mathfrak{R}$ are given volumes, and $w_I, w_J : \Omega \rightarrow \mathfrak{R}^+$ are blur masks obtained from the segmentation of coronary tree structure.

In data fidelity term, we exploit normalized intensity difference in the region of interest as a similarity measure given by:

$$E_{data} = \int_{\Omega} w_I(x) \|I(x) - J \circ h(x)\|^2 dx$$

We can emphasize the coronary tree region using the blur mask as a weighting function that restricts the domain of the similarity measure. Recovering the optimal potential of this objective function is not straightforward. Due to the lack of information, the complete recovery of the local deformation field is an ill-posed problem. The use of regularization is a common practice to overcome this limitation, which means smoothness of the pixel-wise motion field is a natural registration assumption.

The regularization term penalizes the large variation of transformation to ensure the displacement $h(x)$ to be continuous. We adopt so-called diffusion regularization that penalizes the total variation of the flow field, which can be expressed as

$$E_{reg} = \int_{\Omega} \|\nabla h(x)\|^2 dx$$

Finally volume preserving constraint enforces the volume of source coronary tree to be preserved after the registration.

$$E_{vol} = \left(\int_{\Omega} w_J \circ h(x) dx - \int_{\Omega} w_J(x) dx \right)^2$$

2.2 Energy Minimization

The optimal solution to our problem should minimize the following energy:

$$E(x) = \alpha E_{data}(x) + \beta E_{reg}(x) + \lambda E_{vol}(x),$$

where α weights the significance of the data fidelity, β controls the smoothness of segmenting shapes, and λ is a coefficient of the volume-preserving constraint. We found experimentally that $\alpha = 500$, $\beta = 1$, and $\lambda = 0.045$ provide a good compromise between the two terms based on the distance between landmarks described in Section 3.2. A gradient descent is used as a minimization scheme. We omit the detailed derivation of the associated Euler-Lagrange equations due to the space constraints.

3. RESULTS

3.1. Patient Data

3 paired coronary CTA datasets (6 scans in total) obtained on a dual source CT (DSCT) scanner were considered in this retrospective analysis. The imaging protocol has previously been described in detail by Dey et al. [18]. All coronary CTA scans were obtained with the same a 64-slice DSCT scanner (Definition; Siemens Medical Solutions, Arlangen, Germany) with gantry-rotation time of 330 milliseconds and standard detector collimation of 0.6 mm. 80 cc of intravenous contrast was administered before each scan. Raw data were reconstructed using 0.6 mm slice thickness, 0.3 mm slice increment, a 250×250 mm field of view, a transverse field of view encompassing the heart (ranging from 159-241 mm² in the tested datasets), single-segment reconstruction and a medium-smooth reconstruction kernel (B26f). The time difference between baseline and follow-up scans ranged from 4 to 15 months. More detailed patient characteristics and image parameters are described in Table I. The best phase of the cardiac cycle for visualization of coronary arteries was determined by an expert reader at the time of clinical assessment, which ranged from 70% to 80%. The study was conducted according to the guidelines of the Cedars-Sinai Medical Center Institutional Review Board, and all patients gave written informed consent to the retrospective use of their data.

TABLE I
Patient Characteristics and image parameters of baseline and follow-up scans

	Subject 1	Subject 2	Subject 3
Gender	Male	Male	Male
Age	79	64	82
Time Difference	4 months	15 months	11 months
Matrix Size of Baseline (Pixel)	$512 \times 512 \times 417$	$512 \times 512 \times 306$	$512 \times 512 \times 684$
Matrix Size of Follow-up (Pixel)	$512 \times 512 \times 406$	$512 \times 512 \times 404$	$512 \times 512 \times 404$
Pixel Size of Baseline (mm)	$0.43 \times 0.43 \times 0.3$	$0.39 \times 0.39 \times 0.4$	$0.4 \times 0.4 \times 0.29$
Pixel Size of Follow-up (mm)	$0.47 \times 0.47 \times 0.3$	$0.45 \times 0.45 \times 0.3$	$0.45 \times 0.45 \times 0.3$
Cardiac Phase of Baseline	70%	70%	70%
Cardiac Phase of Follow-up	80%	70%	70%

3.2. Validation of Proposed Method

Serial coronary CTA registrations were performed on an Intel Core2 Duo CPU with a clock speed of 2.5 GHz and a 4 GB memory. The mean computation time for the whole process (both global displacement and local deformation) was 5 minutes.

For the initial validation of our proposed algorithm, we obtained anatomical landmarks from each scan including Left Main (LM) artery origin, bifurcation of LM and Left Circumflex (LCX), Right Coronary Artery (RCA) origin and bifurcation of Left Anterior Descending (LAD) and first Diagonal (D1). We measured the difference distance using those points after the registration and the results are presented in Table 2. In Figure 2, we demonstrate the alignment of serial scans with the use of “roving window” technique.

Table 2
Mean distance of anatomical landmarks between registered source and target

	Subject 1	Subject 2	Subject 3	Mean \pm Std
Mean distance (mm)	1.95 ± 0.81	2.01 ± 0.51	2.03 ± 0.67	1.99 ± 0.69

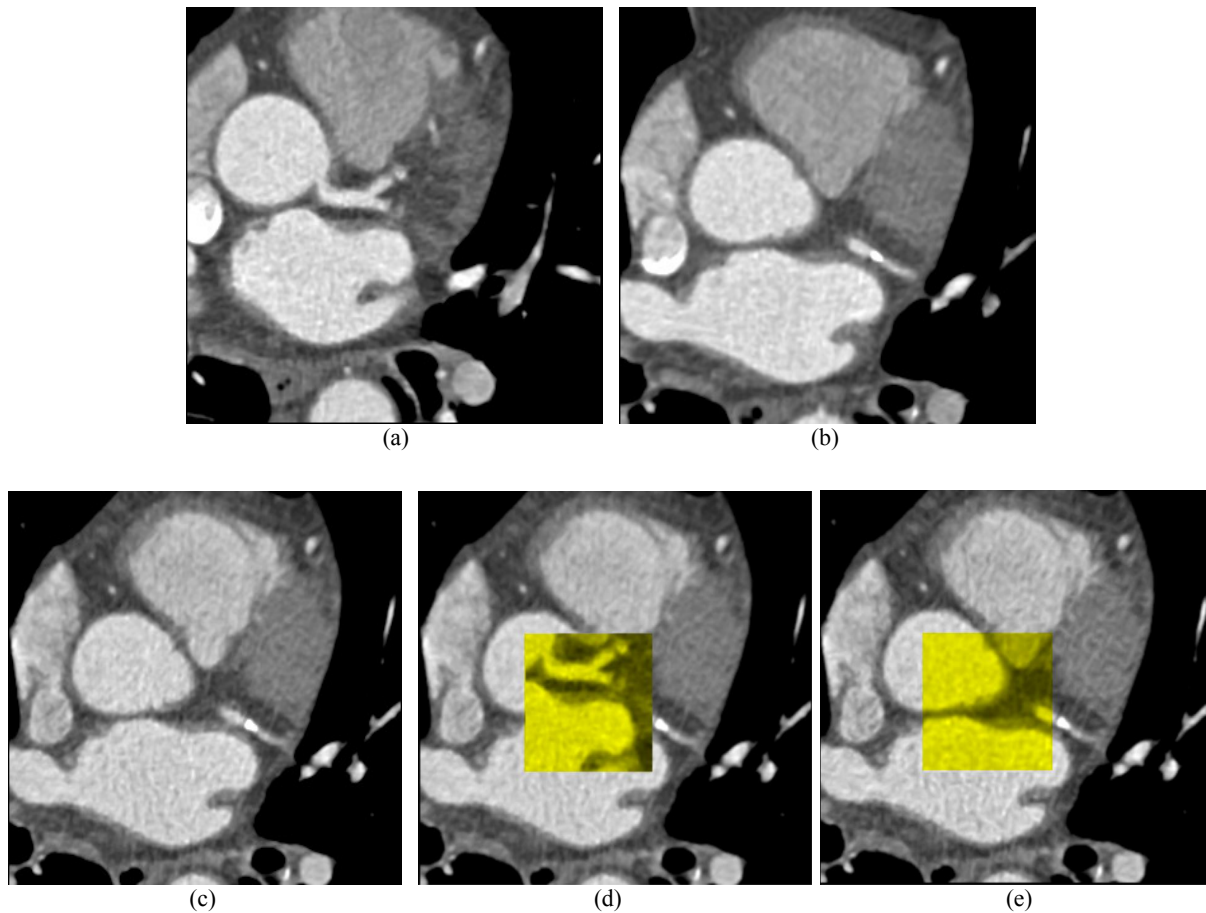


Fig. 3. Example of registration results. Baseline volume is registered to the target volume. The original source image before (a) and after (b) registration is shown. Panel (c) shows the target volume. As shown in (d), original volume is significantly misaligned. The “roving window” (yellow) technique using a portion of the registered image from (b) to the target volume in (c) shown in (e) is a technique to verify the alignment of serial CTA scans.

4. CONCLUSION

We presented an efficient nonlinear 3D volume registration algorithm with “blur mask” generated by the segmentation of coronary trees with novel application to registration of serial coronary CTA scans. This feature mask was used to guide registration and meet a volume preserving constraint. In this paper we proposed a novel registration algorithm in a variational framework. A rigid transformation was performed to find the optimal global displacement based on the segmented coronary tree structures from coronary CTA scans. Then, non-rigid transformation using diffeomorphism was performed to find the optimal local deformations where blur mask was introduced as a weighting function favoring regions of interest given by the segmentation of coronary tree structure. This feature mask was also employed for a volume preserving constraint. The results show accurate registration of serial volumetric coronary CTA scans which has potential of this approach for a clinical application in evaluation of plaque regression and progression from paired coronary CTA scans.

REFERENCES

- [1] Achenbach, S. "Cardiac CT: State of the art for the detection of coronary arterial stenosis." *Journal of Cardiovascular Computed Tomography*, 1(1), 3-20. (2007)
- [2] Berman, D. S., Shaw, L. J., Hachamovitch, R., Friedman, J. D., Polk, D. M., Hayes, S. W., Thomson, L. E. J., Germano, G., Wong, N. D., Xingping, K., and Rozanski, A. "Comparative use of radionuclide stress testing, coronary artery calcium scanning, and noninvasive coronary angiography for diagnostic and prognostic cardiac assessment." *Seminars in Nuclear Medicine*, 37(1), 2-16. (2007)
- [3] Ferencik, M., Ropers, D., Abbara, S., Cury, R. C., Hoffmann, U., Nieman, K., Brady, T. J., Moselewski, F., Daniel, W. G., and Achenbach, S. "Diagnostic accuracy of image postprocessing methods for the detection of coronary artery stenoses by using multidetector CT." *Radiology*, 243(3), 696-702. (2007)
- [4] Edwards, P. J., Hill, D. L., Little, J. A., and Hawkes, D. J. "A three-component deformation model for image-guided surgery." *Med Image Anal*, 2(4), 355-67. (1998)
- [5] Dey, D., Slomka, P. J., Hahn, L. J., and Kloiber, R. "Automatic three-dimensional multimodality registration using radionuclide transmission CT attenuation maps: a phantom study." *J Nucl Med*, 40(3), 448-55. (1999)
- [6] Woo, J., Hong, B. W., Kumar, S., Basu Ray, I., and Kuo, C. C. "Joint Reconstruction and Registration Using Level Sets: Application to the Computer-Aided Ablation of Atrial Fibrillation." *Frontiers in the Convergence of Bioscience and Information Technologies*, Jeju, Korea, 504 - 507.
- [7] Woo, J., Hong, B. W., Kumar, S., Basu Ray, I., and Kuo, C. C. "Multimodal data integration for computer-aided ablation of atrial fibrillation." *J Biomed Biotechnol*, 2008, 681303. (2008)
- [8] Slomka, P. J., Fieno, D., Ramesh, A., Goyal, V., Nishina, H., Thompson, L. E. J., Saouaf, R., Berman, D. S., and Germano, G. "Patient motion correction for multiplanar, multi-breath-hold cardiac cine MR imaging." *Journal of Magnetic Resonance Imaging*, 25(5), 965 - 973. (2007)
- [9] Crum, W. R., Scahill, R. I., and Fox, N. C. "Automated hippocampal segmentation by regional fluid registration of serial MRI: validation and application in Alzheimer's disease." *Neuroimage*, 13(5), 847-855. (2001)
- [10] Hartkens, T., Hill, D. L., Castellano-Smith, A. D., Hawkes, D. J., Maurer, C. R., Jr., Martin, A. J., Hall, W. A., Liu, H., and Truwit, C. L. "Measurement and analysis of brain deformation during neurosurgery." *IEEE Trans Med Imaging*, 22(1), 82-92. (2003)
- [11] Leung, K. K., Holden, M., Saeed, N., Brooks, K. J., Buckton, J. B., Williams, A. A., Campbell, S. P., Changani, K., Reid, D. G., Zhao, Y., Wilde, M., Rueckert, D., Hajnal, J. V., and Hill, D. L. "Automatic quantification of changes in bone in serial MR images of joints." *IEEE Trans Med Imaging*, 25(12), 1617-26. (2006)
- [12] Rey, D., Subsol, G., Delingette, H., and Ayache, N. "Automatic detection and segmentation of evolving processes in 3D medical images: Application to multiple sclerosis." *Medical Image Analysis*, 6(2), 163-179. (2002)
- [13] Mackie, T. R., Kapatoes, J., Ruchala, K., Lu, W., Wu, C., Olivera, G., Forrest, L., Tome, W., Welsh, J., Jeraj, R., Harari, P., Reckwerdt, P., Paliwal, B., Ritter, M., Keller, H., Fowler, J., and Mehta, M. "Image guidance for precise conformal radiotherapy." *Int J Radiat Oncol Biol Phys*, 56(1), 89-105. (2003)
- [14] Shi, J., Sahiner, B., Chan, H. P., Hadjiiski, L., Zhou, C., Cascade, P. N., Bogot, N., Kazerooni, E. A., Wu, Y. T., and Wei, J. "Pulmonary nodule registration in serial CT scans based on rib anatomy and nodule template matching." *Med Phys*, 34(4), 1336-47. (2007)
- [15] Slomka, P. J., and Baum, R. P. "Multimodality image registration with software: state-of-the-art." *Eur J Nucl Med Mol Imaging*. (2008)
- [16] Takao, H., Doi, I., and Tateno, M. "Evaluation of an automated system for temporal subtraction of thin-section thoracic CT." *Br J Radiol*, 80(950), 85-9. (2007)
- [17] Wang, H., Dong, L., O'Daniel, J., Mohan, R., Garden, A. S., Ang, K. K., Kuban, D. A., Bonnen, M., Chang, J. Y., and Cheung, R. "Validation of an accelerated 'demons' algorithm for deformable image registration in radiation therapy." *Phys Med Biol*, 50(12), 2887-905. (2005)
- [18] Dey, D., Lee, C. J., Ohba, M., Gutstein, A., Slomka, P. J., Cheng, V., Suzuki, Y., Suzuki, S., Wolak, A., Le Meunier, L., Thomson, L. E. J., Cohen, I., Friedman, J. D., Germano, G., and Berman, D. S. "Image quality and artifacts in coronary CT angiography with dual-source CT: Initial clinical experience." *Journal of Cardiovascular Computed Tomography*, 2(2), 105-114. (2008)